Mammalian Mst1 and Mst2 kinases play essential roles in organ size control and tumor suppression

Hai Song[a,1], Kinglun Kingston Mak[a,1], Lilia Topol[a], Kangsun Yun[a], Jianxin Hu[a], Lisa Garrett[a], Yongbin Chen[b], Ogyi Park[c], Jia Chang[d], R. Mark Simpson[e], Cun-Yu Wang[d], Bin Gao[c], Jin Jiang[b], and Yingzi Yang[a,2]

[a]Genetic Disease Research Branch, National Human Genome Research Institute, Bethesda, MD 20892; [b]Departments of Developmental Biology and Pharmacology, UT Southwestern Medical Center, Dallas, TX 75390-9133; [c]Section on Liver Biology, National Institute on Alcohol Abuse and Alcoholism, Bethesda, MD 20892; [d]Division of Oral Biology and Medicine, UCLA School of Dentistry, Los Angeles, CA 90095-1668; and [e]Laboratory of Cancer Biology and Genetics, National Cancer Institute, Bethesda, MD 20892

Edited by Clifford J. Tabin, Harvard Medical School, Boston, MA, and approved December 7, 2009 (received for review October 5, 2009)

Control of organ size by cell proliferation and survival is a fundamental developmental process, and its deregulation leads to cancer. However, the molecular mechanism underlying organ size control remains elusive in vertebrates. In *Drosophila*, the Hippo (Hpo) signaling pathway controls organ size by both restricting cell growth and proliferation and promoting cell death. Here we investigated whether mammals also require the Hpo pathway to control organ size and adult tissue homeostasis. We found that *Mst1* and *Mst2*, the two mouse homologs of the *Drosophila Hpo*, control the sizes of some, but not all organs, in mice, and *Mst1* and *Mst2* act as tumor suppressors by restricting cell proliferation and survival. We show that *Mst1* and *Mst2* play redundant roles, and removal of both resulted in early lethality in mouse embryos. Importantly, tumors developed in the liver with a substantial increase of the stem/progenitor cells by 6 months after removing *Mst1* and *Mst2* postnatally. We show that Mst1 and Mst2 were required in vivo to control Yap phosphorylation and activity. Interestingly, apoptosis induced by TNFα was blocked in the *Mst1* and *Mst2* double-mutant cells both in vivo and in vitro. As TNFα is a pleiotropic inflammatory cytokine affecting most organs by regulating cell proliferation and cell death, resistance to TNFα-induced cell death may also contribute significantly to tumor formation in the absence of *Mst1* and *Mst2*.

Hippo signaling | tumor suppressor | Yap phosphorylation

During development and regeneration, the determinants of vertebrate organ size are poorly understood, but include extrinsic and intrinsic factors that coordinate cell proliferation and cell death (1–4). Recent studies in *Drosophila* suggest that the Hippo (Hpo) signaling pathway plays an important role in organ size control (5, 6). Central to the Hpo pathway is a kinase cascade consisting of Hpo, Salvador (Sav), Warts (Wts), and Mats (6, 7). Mutations in any of these genes resulted in overgrowth of adult appendages, including eyes and wings (8–16). Hpo, also called dMst (9), is the *Drosophila* homolog of mammalian Ste20 family kinases Mst1 and Mst2, and forms a complex with the WW-repeat scaffolding protein Sav to phosphorylate and activate the downstream kinase Wts/Lats. Wts/Lats acts in association with a small regulatory protein Mats to restrict cell growth and proliferation and promote cell death primarily by regulating Yorkie (Yki), the *Drosophila* homolog of mammalian transcriptional coactivator YAP and TAZ (17–19). Hpo/Wts-mediated phosphorylation of Yki restricts its nuclear localization (20–22), and Yki interacts with the TEAD/TEF family transcription factor Scalloped (Sd) to regulate Hpo pathway target genes (21, 23, 24).

The Hpo pathway is evolutionarily conserved, and the vertebrate Hpo pathway has been implicated in regulating cell contact inhibition, organ size, and tumorigenesis (6, 7). Yap is the primary effector of the mammalian Hpo pathway (20, 25–27). YAP in human is a candidate oncogene that is amplified in several types of tumor (28, 29). YAP protein levels and/or nuclear localization are elevated in many human cancers (20, 30). Yap nuclear localization can be regulated by cell-cell contact through Lats-mediated phosphorylation (20, 25). Overexpression of an activated and nuclear localized form of Yap in mouse liver increased liver size (20, 26), which ultimately resulted in hepatocellular carcinoma (20). As in *Drosophila*, the TEAD family of transcription factors mediates the function of Yap and Taz in mammalian cells (31–34).

Here we have addressed the physiological role of the mammalian Hpo pathway mediated by *Mst1* and *Mst2* during embryonic development and adult tissue homeostasis by genetically removing *Mst1* and *Mst2* in mouse embryos and adult tissues. We found that *Mst1* and *Mst2* play redundant roles and are required for mouse embryonic development, size control of some organs, and tumor suppression. We also provide evidence that resistance to TNFα-induced cell death may contribute significantly to tumor formation in the absence of *Mst1* and *Mst2*.

DEVELOPMENTAL BIOLOGY

Results

***Mst1* and *Mst2* Play Redundant Roles in Mammalian Embryonic Development.** To investigate the function of the mammalian Hpo signaling pathway in vivo (6, 7), we generated conditional alleles of *Mst1* ($Mst1^c$) and *Mst2* ($Mst2^c$). The mutant $Mst1^{\Delta}$ and $Mst2^{\Delta}$ alleles were derived from the conditional alleles using the *Sox2-Cre* line (35) (Fig. S1*A*). Because the sequences encoding the kinase domains were deleted in the $Mst1^{\Delta}$ and $Mst2^{\Delta}$ alleles, and Mst1 and Mst2 proteins were not detected in the $Mst1^{\Delta/\Delta}$ and $Mst2^{\Delta/\Delta}$ embryos (Fig. S1*B*), the $Mst1^{\Delta}$ and $Mst2^{\Delta}$ are null alleles. The $Mst1^{\Delta/\Delta}$ and $Mst2^{\Delta/\Delta}$ mice were viable, morphologically normal, and fertile. This is due to the functional redundancy of *Mst1* and *Mst2* in embryonic development as the $Mst1^{\Delta/\Delta};Mst2^{\Delta/\Delta}$ mice were embryonically lethal (Table S1 and Fig. S2). The double-mutant embryos were reduced in size, developmentally delayed, and died between E9.5 and 11.5 (Table S2 and Fig. S2*A*), possibly due to hematopoietic defects, because the yolk sac and the embryo were very pale compared with the control (Fig. S2*B*). The $Mst1^{\Delta/\Delta};Mst2^{\Delta/+}$ and $Mst1^{\Delta/+};Mst2^{\Delta/\Delta}$ mice were also viable, morphologically normal, and fertile. These findings suggest that *Mst1* and *Mst2* play redundant and essential roles in early embryonic development, and that one copy of either *Mst1* or *Mst2* is sufficient to support normal embryonic development.

Author contributions: H.S., K.K.M., and Y.Y. designed research; H.S., K.K.M., L.T., K.Y., J.H., L.G., Y.C., O.P., J.C., and Y.Y. performed research; H.S., L.G., and B.G. contributed new reagents/analytic tools; H.S., K.K.M., L.T., K.Y., J.H., Y.C., R.M.S., C.-Y.W., J.J., and Y.Y. analyzed data; and Y.Y. wrote the paper.

The authors declare no conflict of interest.

This article is a PNAS Direct Submission.

[1]H.S. and K.K. contributed equally to this work.

[2]To whom correspondence should be addressed at: Genetic Disease Research Branch, National Human Genome Research Institute, 49 Convent Drive, Bethesda, MD 20892-4472. E-mail: yingzi@mail.nih.gov.

This article contains supporting information online at www.pnas.org/cgi/content/full/0911409107/DCSupplemental.

We then examined Yap phosphorylation in primary mouse embryonic fibroblast (MEF) cells and hepatocytes. Yap phosphorylation was significantly reduced when *Mst1* and *Mst2* were removed in hepatocytes, but not in MEF cells (Fig. S1*C*). Using a TEAD/Sd luciferase reporter (21), however, we found that the transcriptional activity of Yap was increased in the *Mst1*/*Mst2* MEF cells (Fig. S1*D*), suggesting that *Mst1* and *Mst2* may be required differentially for Yap phosphorylation and TEAD activity inhibition in vivo.

***Mst1* and *Mst2* Regulate the Size of Certain Organs.** Because early lethality of the $Mst1^{\Delta/\Delta};Mst2^{\Delta/\Delta}$ mutant embryos precludes the assessment of the role of *Mst1* and *Mst2* at later stages of development, particularly in regulating mammalian organ size and tissue homeostasis, we employed tissue-specific *Cre* lines to remove *Mst1* and *Mst2* in specific organs. Surprisingly, when *Mst1* and *Mst2* were removed from the developing limb mesoderm by the *Prx1-Cre* (36) (Fig. S3 *A* and *B*), the limb was actually shorter with shorter skeletal elements (Fig. S3*C*). However, there were no obvious defects in skeletal development (Fig. S3*D*) except that the cell size appeared to be smaller and cell density was increased in the cartilage of the $Mst1^{\Delta/\Delta};Mst2^{c/\Delta}$;*Prx1-Cre* embryo (Fig. S3 *D* and *E*). Chondrocyte proliferation, as examined by Ki67 expression, was significantly increased in the mutant embryo (Fig. S3*F*). Interestingly, in the mutant, Ki67 staining was also detected in the enlarged hypertrophic chondrocytes, which had exited cell cycle and undergone terminal differentiation in the control embryo. Thus, the mammalian Hpo signaling pathway is not required for hypertrophic differentiation of chondrocytes, but is required for these cells to exit cell cycle during hypertrophy. Cell death examined by the TdT-mediated dUTP nick end labeling (TUNEL) assay was detected in the hypertrophic chondrocytes at the chondro-osseous junction in the control embryo, whereas in the mutant, it was reduced (Fig. S3*G*). Despite increased cell proliferation and reduced cell death, the cartilage size of the mutant was not increased, indicating that cell proliferation and death are not the only determining factors in vertebrate organ size control.

To test whether loss of *Mst1* and *Mst2* can lead to increased sizes in other organs, we removed *Mst1* and *Mst2* in all organs in newborn mouse pups with the tamoxifen (TM)-inducible *CAGGCre-ER* line (37). Injecting TM into the mouse pups induced substantial gene deletion in the liver, stomach, small intestine, skin, lung, heart, spleen, and kidney when assessed by molecular analyses and the *R26R* mouse line (38) (Fig. S3 *H–J*). No obvious change was observed in the size of total body, limb, and skeleton in the $Mst1^{\Delta/\Delta};Mst2^{c/\Delta}$;*CAGGCre-ER* mice. However, the liver and stomach were always enlarged 1–7 months after TM-induced gene inactivation. The heart and spleen were also enlarged, albeit less frequently. We never observed enlarged lung, kidney, and intestines ($n = 8$). Furthermore, removing *Mst1* and *Mst2* specifically in the liver by the *Albumin-Cre* (39) resulted in significant liver enlargement and dysplasia at 1 month of age (Fig. 1*A*). Hepatocytes in the mutant were smaller and cell densities were higher. Some cells showed vacuolated cytoplasm (Fig. 1*B*). Cell proliferation was increased (Fig. 1*C*), but cell death was only slightly increased in the mutant liver (Fig. 1*D*). These findings suggest that *Mst1* and *Mst2* are required to restrict cell proliferation, but their control of organ size is tissue specific in mammals.

Loss of *Mst1* and *Mst2* Leads to Tumor Formation in the Liver. To test whether increased cell proliferation in the absence of *Mst1* and *Mst2* eventually led to tumor formation, we let the TM-injected $Mst1^{\Delta/\Delta};Mst2^{c/\Delta}$;*CAGGCre-ER* mice and their wild-type littermate mice age. By 6 months, liver tumors developed in all $Mst1^{\Delta/\Delta};Mst2^{c/\Delta}$;*CAGGCre-ER* mice (6/6) (Fig. 2*A*). No tumor was found in the heart, lung, kidney, small intestine, or skin. In addition, all TM-injected wild-type mice were normal and tumor free. The liver tumor nodules displayed characteristics of hepatocellular carcinoma (HCC). The cells in the nodule exhibited abnormal hematoxylin and eosin (H&E) staining, cellular pleiomorphism (some enlarged cells were mixed with small cells), and/or loss of cytoplasmic staining (Fig. 2*B*). In some liver tumor samples, cholangiocarcinoma (CC), composed of mainly multilayered biliary epithelial cells, was also found (Fig. 2*B*). Significantly increased cell proliferation was found in the liver of the $Mst1^{\Delta/\Delta};Mst2^{c/\Delta}$;*CAGGCre-ER* mice (Fig. 3*A*). However, cell death was also increased in the liver tumors (Fig. 3*B*), possibly secondary to cell overproliferation. These findings suggest that *Mst1* and *Mst2* suppress tumors by restricting cell proliferation. To test whether tumors form spontaneously as a result of loss of heterozygosity of *Mst1* or *Mst2*, we let the $Mst1^{\Delta/\Delta};Mst2^{c/\Delta}$, $Mst1^{\Delta/\Delta};Mst2^{c/c}$ mice and their $Mst1^{\Delta/+};Mst2^{\Delta/+}$ control littermates age ($n > 30$). By 12 months, only liver tumors were found in the $Mst1^{\Delta/\Delta};Mst2^{c/\Delta}$ mice (2/31) (Fig. S4*A*). Because Mst2 could not be detected in the tumor nodules in the $Mst1^{\Delta/\Delta};Mst2^{c/\Delta}$ liver, the tumor likely resulted from loss of *Mst2* heterozygosity in the absence of *Mst1* (Fig. S5*B*). These findings show that *Mst1* and *Mst2* are potent tumor suppressors, in the absence of which liver tumors form preferentially.

Because expression of an active form of Yap (YapS127A) leads to increased liver size and ultimately liver tumor formation (20), we tested whether increased cell proliferation and tumor formation in the liver of the $Mst1^{\Delta/\Delta};Mst2^{c/\Delta}$;*CAGGCre-ER* mice are associated with reduced Yap phosphorylation by analyzing liver samples with immunohistochemistry and Western blots. YAP protein levels

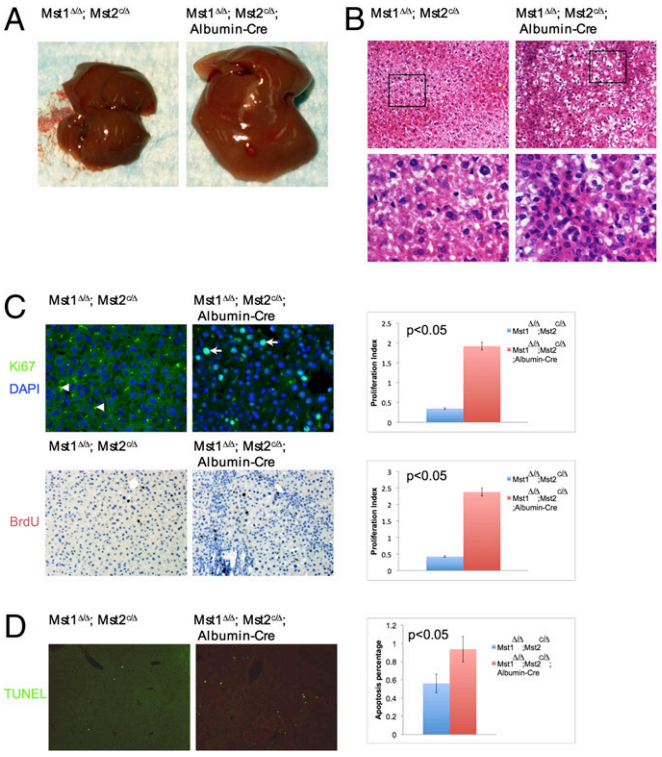

Fig. 1. Removal of *Mst1* and *Mst2* in the liver. (*A*) Livers from 1-month-old mice. (*B*) H&E staining of liver sections. The boxed region is shown in higher magnification in the lower panel. The cells in the $Mst1^{\Delta/\Delta};Mst2^{c/\Delta}$;*Albumin-Cre* liver were smaller and the density was higher. (*C*) Cell proliferation shown by Ki67 (green, arrow) and BrdU staining (brown, *Lower*). More Ki67- or BrdU-positive cells were found in the $Mst1^{\Delta/\Delta};Mst2^{c/\Delta}$;*Albumin-Cre* liver. Autofluorescence blood cells were indicated by arrowhead. (*Right*) Statistical analysis. (*D*) TUNEL assay of liver sections. A slight increase in cell death (arrow) was detected in the mutant liver as quantified in the right panel.

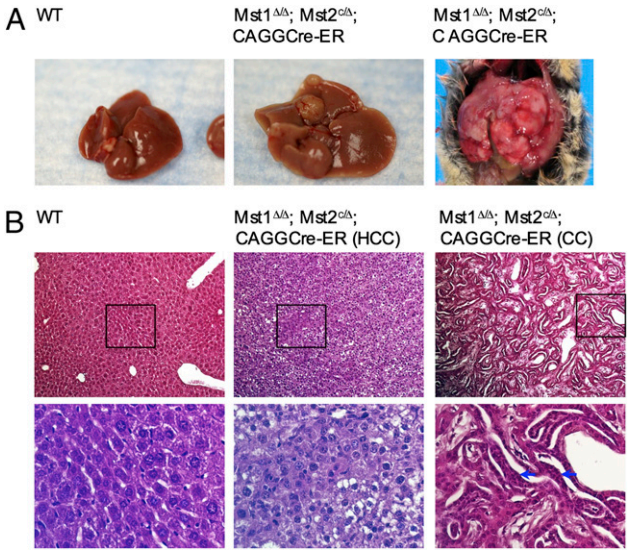

Fig. 2. Liver tumors form in the absence of Mst1 and Mst2. (*A*) Livers from 6-month-old TM-injected wild-type and mutant mice. Two of the mutant livers with tumor nodules are shown. (*B*) H&E staining of liver sections from the liver samples in *A*. Boxed regions are shown in the lower panel in higher magnification. Both hepatocyte carcinoma (HCC) and chonlangiocyte carcinoma (CC) were observed. Multilayered epithelial cells are indicated by arrows.

were increased and Yap phosphorylation was significantly reduced in the primary $Mst1^{\Delta/\Delta};Mst2^{\Delta/\Delta}$ hepatocytes and liver tumor nodules (Fig. S1*C* and Fig. 3*C*). In addition, Yap nuclear localization was increased in pretumor hepatocytes (Fig. 3*E*) and liver tumor nodules (Fig. 3*D* and Fig. S4*B*).

Cellular and Molecular Alterations in the *Mst1* and *Mst2* Mutant Liver. To understand the molecular mechanism underlying tumor formation in the absence of *Mst1* and *Mst2*, we examined expression of genes implicated in Yap-regulated proliferation and cell death in the liver (21). In both the liver tumor nodules and pretumor mutant liver samples (Fig. S4 *C* and *D*), *Survivin* mRNA expression was significantly up-regulated. We did not observe consistent up-regulation of *cMyc*, *cIAP*, and *Sox4* expression. Interestingly, we also found that in the liver tumor nodules and pretumor mutant liver tissue, β-catenin levels were increased and nuclear localization of β-catenin was observed (Fig. S4 *E* and *F*). In addition, loss of *Mst1* and *Mst2* led to increased β-catenin transcription activity in the MEF cells (Fig. S4*G*). These findings suggest that the Wnt/β-catenin signaling activity, which is oncogenic by itself (40–42), was also increased in the absence of *Mst1* and *Mst2*.

The presence of both HCC and CC in the liver of $Mst1^{\Delta/\Delta};Mst2^{c/\Delta}$; *CAGGCre-ER* mice suggests that these tumors may have originated from liver progenitor cells that give rise to both hepatocytes and cholangiocytes (biliary epithelial cells). When a stem/progenitor cell on its way to differentiation develops into cancer, this will give rise to tumors with a full range of phenotypes with varying hepatocellular and cholangiacellular differentiation characteristics (43). Liver stem cell/progenitor cells are hard to find in the wild-type adult liver, and they express cytokeratin 19 (CK-19) and alpha-fetoprotein (AFP) (43–47). However, in the liver of the $Mst1^{\Delta/\Delta};Mst2^{c/\Delta};CAGGCre\text{-}ER$ mice, the number of CK-19- and AFP-expressing cells was dramatically increased (Fig. S4*H*), suggesting

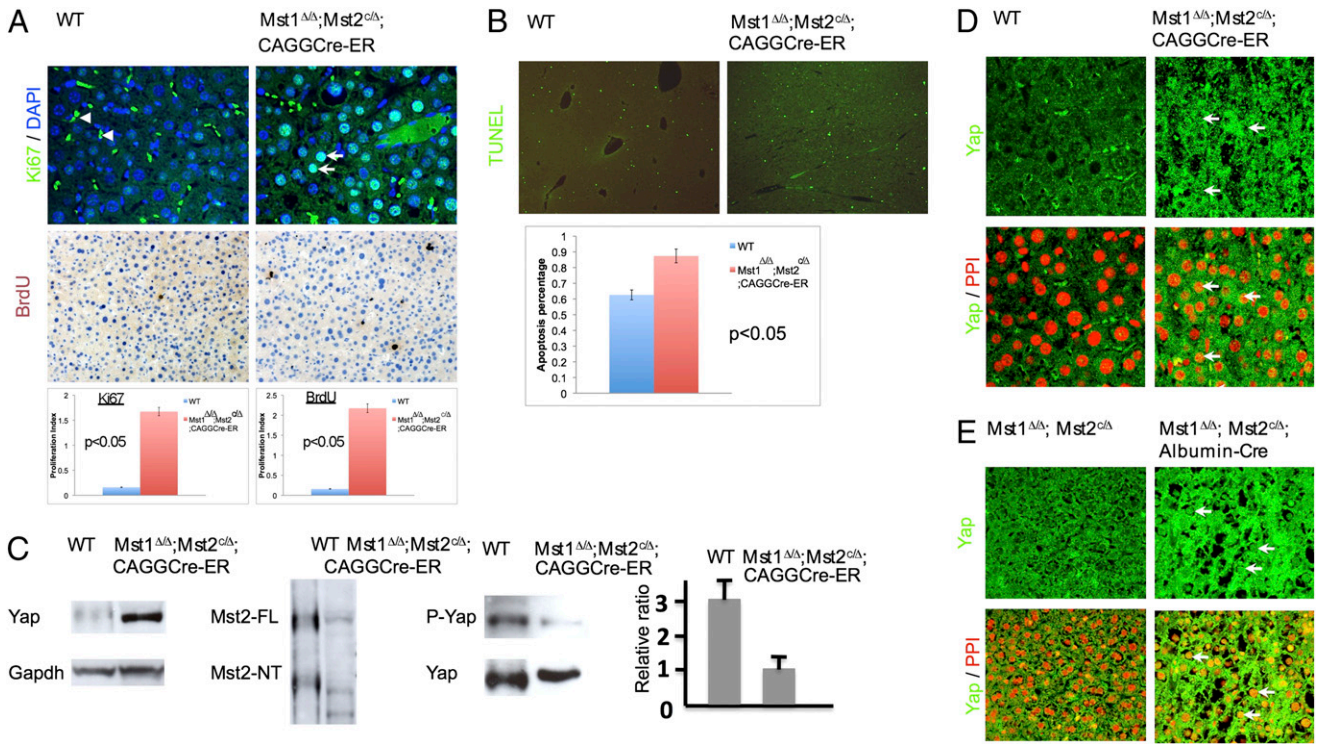

Fig. 3. Increased cell proliferation and reduced Yap phosphorylation in the liver tumor. (*A*) Ki67 (green) and BrdU staining (brown) of liver sections from 6-month-old TM-injected wild-type and $Mst1^{\Delta/\Delta};Mst2^{c/\Delta};CAGGCre\text{-}ER$ mice. In the HCC regions, both Ki67- and BrdU-positive cell numbers were increased as shown by quantification. DAPI (blue) stains the nucleus. Autofluorescence blood cells were indicated by arrowhead. (*B*) TUNEL assay of liver sections as in *A*. Cell death (green) was increased in the HCC region as shown by quantification. (*C*) Western blot of samples from normal (wild-type) and tumor ($Mst1^{\Delta/\Delta};Mst2^{c/\Delta};CAGGCre\text{-}ER$)-bearing livers. GAPDH was control for total protein, and Yap phosphorylation levels were normalized by the total Yap protein. The phosphorylated YAP to total YAP protein ratio was significantly reduced in the mutant as quantified by densitometry. (*D* and *E*) Immunohistochemistry of Yap (green) on the liver sections. Yap protein levels and nuclear localization (arrow) were increased in the mutants. (*Lower*) Nucleus stained red by propidium iodide (PPI, red).

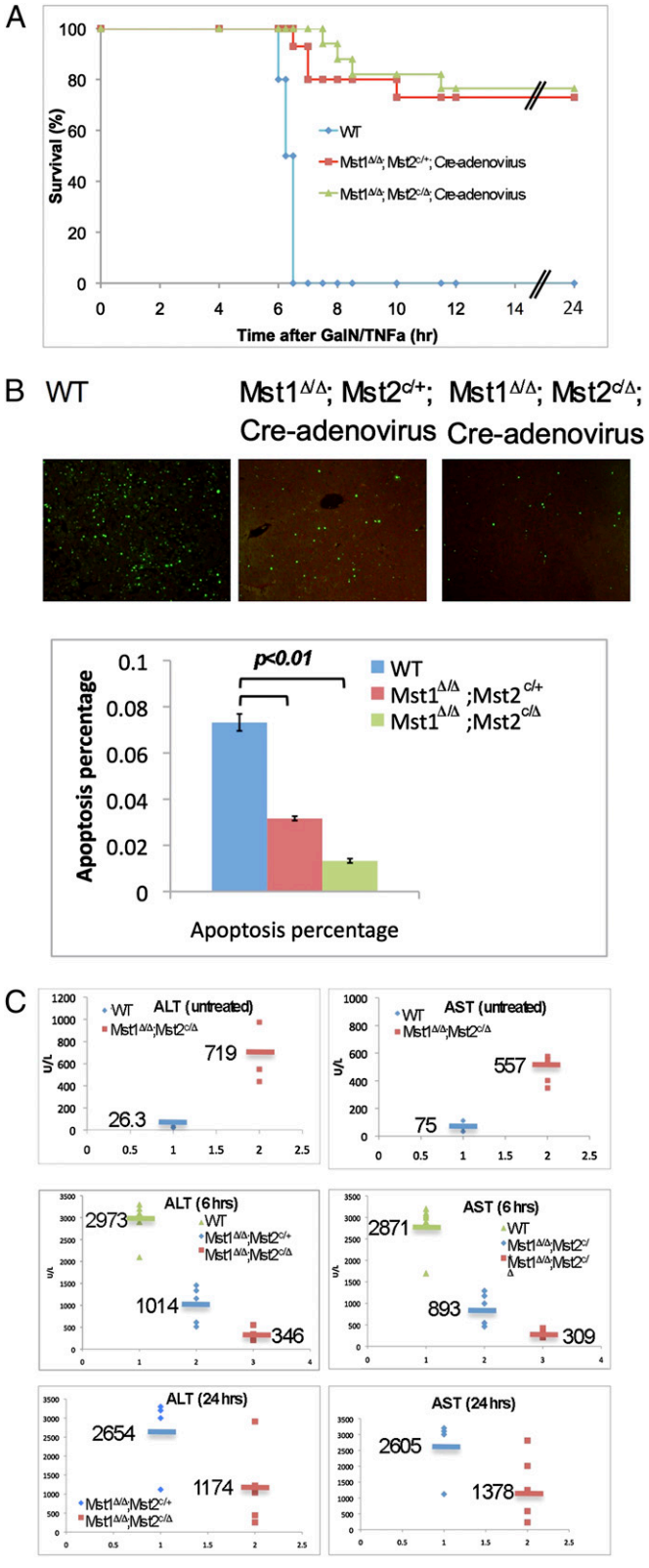

Fig. 4. TNFα-induced liver toxicity was blocked by loss of *Mst1* and *Mst2*. (*A*) Survival of *Cre-adenovirus*-injected wild-type mice ($n = 10$), $Mst1^{\Delta/\Delta};Mst2^{c/+}$ mice ($n = 10$), and $Mst1^{\Delta/\Delta};Mst2^{c/\Delta}$ mice ($n = 10$) after treatment with GalN and TNFα. (*B*) TUNEL analysis of liver tissue isolated 6 h after administration of GalN and TNFα. Results represent the staining of four mice from each group. (*C*) Serum concentration of liver enzymes in nontreated mice or at 6 h and 24 h after treatment with GalN and TNFα ($n = 5$ mice per group). ALT, alanine aminotransferase; AST, aspartate aminotransferase.

that the HCCs and CCs might result from overproliferation of the stem/progenitor cells.

Loss of *Mst1* and *Mst2* Renders Liver Resistant to TNFα-Induced Apoptosis. As cytokines like TNFα play very important roles in regulating hepatocyte proliferation and survival (48, 49), and loss of *Mst1* and *Mst2* led to liver tumor formation preferentially, we examined TNFα response in the *Mst1* and *Mst2* mutant cells. Both $Mst1^{\Delta/\Delta};Mst2^{\Delta/\Delta}$ MEF cells and hepatocytes were resistant to TNFα-induced cell death (Fig. S5*A*). In support of this, we found that in both MEF cells and hepatocytes, TNFα-induced JNK activation was weakened and AKT activation was prolonged, suggesting that JNK and AKT activation by TNFα in regulating cell death might, to a certain extent, requires *Mst1* and *Mst2* (Fig. S5 *B* and *C*). Other immediate readouts of TNFα signaling, including IκB degradation, were normal (Fig. S5*D*).

To test whether loss of *Mst1* and *Mst2* renders liver resistant to TNFα-induced cell death, we first removed the *Mst1* and *Mst2* in the liver by injecting the *Cre-adenovirus* into the $Mst1^{\Delta/\Delta};Mst2^{c/\Delta}$, $Mst1^{\Delta/\Delta};Mst2^{c/+}$ and wild-type mice. The adenovirus preferentially infects the liver as shown by the injected *GFP-adenovirus* (Fig. S6*A*). Acute liver cell death was induced in vivo by injecting TNFα to mice (50). Though all wild-type mice died by 6.5 h postinjection (PI), all $Mst1^{\Delta/\Delta};Mst2^{c/\Delta}$ littermates were completely protected from TNFα-induced liver injury and appeared healthy until 24 h or even 2 months PI (Fig. 4*A*). Interestingly, most of the $Mst1^{\Delta/\Delta};Mst2^{c/+}$ mice also survived at 24 h PI and appeared to be healthy (Fig. 4*A*). Apoptosis was strongly increased in the wild-type livers, but significantly and progressively reduced in the $Mst1^{\Delta/\Delta};Mst2^{c/+}$ and $Mst1^{\Delta/\Delta};Mst2^{c/\Delta}$ livers (Fig. 4*B*). Higher circulating concentrations of alanine aminotransferase (ALT) and aspartate aminotransferase (AST) in wild-type mice at 6 h PI confirmed the development of liver injury (Fig. 4*C*). The $Mst1^{\Delta/\Delta};Mst2^{c/\Delta}$ mice had ALT and AST levels similar to those of untreated ones, whereas the AST and ALT levels in the $Mst1^{\Delta/\Delta};Mst2^{c/+}$ mice were only slightly increased (Fig. 4*C*). By 24 h PI, the AST and ALT levels were much higher in the $Mst1^{\Delta/\Delta};Mst2^{c/+}$ mice (Fig. 4*C*). Therefore, the deletion of *Mst1* and *Mst2* rendered mice resistant to TNFα cytotoxicity in a gene-dose dependent manner. We also notice that the AST and ALT levels in the untreated $Mst1^{\Delta/\Delta};Mst2^{c/\Delta}$ mice were higher than those in the wild-type control mice (Fig. 4*C*), suggesting that there was liver inflammation in the $Mst1^{\Delta/\Delta};Mst2^{c/\Delta}$ mice.

The requirement of *Mst1* and *Mst2* in promoting cell death was further confirmed by activating the death receptor Fas, a potent inducer of liver apoptosis, through injecting the Jo-2 antibody, a Fas agonist (51–53). All wild-type control mice died by 4.5 h PI, whereas all $Mst1^{\Delta/\Delta};Mst2^{c/\Delta}$ and $Mst1^{\Delta/\Delta};Mst2^{c/+}$ mutant mice survived beyond 16 h PI (Fig. S6*B*). Again, cell death was massive in the wild-type liver, but much reduced in the $Mst1^{\Delta/\Delta};Mst2^{c/\Delta}$ and $Mst1^{\Delta/\Delta};Mst2^{c/+}$ mutant liver (Fig. S6*C*). Taken together, these findings suggest that *Mst1* and *Mst2* are required to promote cell death triggered by external signals such as TNFα in vivo.

Discussion

Here we show that the mammalian *Hpo* homologs *Mst1* and *Mst2* are required to control cell proliferation and cell death in both embryonic development and adult tissue homeostasis. Loss of *Mst1* and *Mst2* leads to increased organ size and tumor formation preferentially in the liver. *Mst1* and *Mst2* are potent tumor suppressor genes; a single copy of either *Mst1* or *Mst2* can significantly inhibit tumor formation in the liver.

How appropriate organ sizes are achieved and maintained in development and tissue repair or regeneration is a question that has fascinated many biologists. Organ sizes are controlled by both intrinsic and extrinsic factors, and it is conceivable that extrinsic factors need to act through intrinsic pathways. *Mst1* and *Mst2* are key players in a critical intracellular signaling pathway controlling cell proliferation and cell death during organ size control and

tumorigenesis. Whether Mst1 and Mst2 activities are controlled by extracellular cues or whether they are constitutively active intrinsic regulators remains elusive. In *Drosophila*, the atypical cadherin Fat (Ft) has been identified as a potential receptor regulating the Hpo pathway (54–56). However, in mammalian cells, the role of *Fat*s in regulating tissue growth has not been demonstrated. Here we have identified cytokines like TNFα as critical extracellular cues that may act through the mammalian Hpo pathway to regulate cell death. These findings also suggest that *Mst1* and *Mst2* may play important roles regulating inflammation.

It is important to note that when *Mst1* and *Mst2* were removed by ubiquitously expressed inducible Cre recombinase, not all organs increased their sizes. Organ sizes are determined by at least the following factors: cell number, size, and density. It has been shown that different vertebrate organs employ distinct mechanisms to control organ sizes (57). For instance, the pancreas organ size is determined by the number of progenitor cells that are set aside early in development, whereas the liver size is not constrained by the early progenitor cell numbers. In both liver and cartilage, we observed reduced cell size and increased cell density when cell proliferation was increased. Thus, it appears that organs can offset the impact of cell number changes on final organ sizes by altering cell size and density, although the underlying feedback mechanism is not clear. In the cartilage, such feedback mechanism is so robust such that the final cartilage is even smaller in the *Mst1* and *Mst2* mutant limb. In addition, vertebrate organs are more complex in that each organ is composed of a distinct set of different cell types. Interactions among these different cell types also contribute significantly to final organ size. For instance, the limb size is controlled by epithelial-mesenchymal interactions mediated by factors such as the fibroblast growth factors (Fgfs) (58, 59). Such interactions may also be subject to feedback regulations when cell proliferation or cell death is intrinsically altered, for instance, by loss of *Mst1* and *Mst2*.

The rapid development of liver tumor caused by loss of *Mst1* and *Mst2* or Yap overactivation suggests that Yap is a primary effector of the mammalian Hpo signaling pathway in vivo. Intriguingly, Yap phosphorylation was much less dependent on *Mst1* and *Mst2* in MEF cells than in hepatocytes, suggesting that Yap phosphorylation does not entirely depend on *Mst1* and *Mst2*. In mice, other Ste20 kinase family members that have lower sequence homologies to Hpo outside of the kinase domain may also phosphorylate YAP, albeit less efficiently. Tissue-specific regulation of Yap phosphorylation and Yap activity may explain why tumors form more quickly in the liver than in other organs, such as the intestine (Fig. S7).

HCC is the fifth most frequent cancer worldwide and the third leading cause of cancer death due to the lack of effective treatment options (60). Surgical removal or liver transplantation is the only curative treatments for HCC, but neither is applicable to most patients with advanced disease. Liver cancer may respond differently from other cancers to standard treatments because of the intrinsic regenerative ability of the liver. The development of HCC and CC is invariably associated with chronic liver damages that can target liver progenitor cells, leading to their expansion and transformation (43, 61). HCCs expressing progenitor cell markers like CK-19 have a more aggressive clinical course. Some studies show that even 5% CK-19 positive cells already affect the outcome of the patient (43). Thus, determining the precise cellular origin of liver tumors is critical in developing the most effective therapeutic strategies. Importantly, we have identified Hpo signaling pathway as a significant target in treating aggressive liver tumors. First, the liver tumors formed in the *Mst1* and *Mst2* mutants are likely to be caused by increased proliferation of liver stem/progenitor cells that can give rise to both hepatocytes and cholangiocytes. Second, *Mst1* and *Mst2* mutant cells are resistant to TNFα-induced cell death. TNFα is a major cytokine/growth factor in the liver that promotes liver progenitor cell growth, and it is produced during inflammation and partial hepatectomy (PH) (47). It is conceivable that loss of cell death response to TNFα will significantly augment its proproliferation effect in liver tumorigenesis.

Materials and Methods

Mouse Strains. The *Sox2-cre* (35), *CAGGCre-ER* (37), and *R26R* (38) mouse lines have been described previously. Genotyping was done by PCR using genomic DNA prepared from the mouse yolk sac or tail.

Tamoxifen (TM) Induction in Mice. TM (Sigma) was dissolved in corn oil (Sigma) at a concentration of 30 mg/mL. A single dose of tamoxifen (0.2 mg/g body weight) was injected intraperitoneally at postnatal day 10 (P10). Organ samples were fixed in 4% paraformaldehyde overnight at 4 °C and embedded in paraffin and sectioned at 6 μm thickness.

Histological Analysis and Western Blot. Primary antibodies used in immunohistochemistry include anti-Ki67 mouse monoclonal IgG (Dako) at 1:50, anti-Yap rabbit polyclonal IgG (Santa Cruz) at 1:50, anti-phospho-Yap rabbit polyclonal IgG (Cell Signaling) at 1:50, anti-β-catenin mouse monoclonal IgG (Transduction Lab), anti-Mst2 rabbit polyclonal IgG (Cell Signaling) at 1:50, anti-CK-19 mouse IgG (Dako) at 1:50, and anti-AFP goat IgG (Dako) at 1:25. The signal was detected using FITC-conjugated secondary antibodies (Molecular Probes). Apoptosis was detected as described (62). Additional antibodies used in Western blot: anti-JNK (BD Pharmingen); anti-phospho-JNK (Cell Signaling); anti-Akt and anti-phospho-Akt (Cell Signaling); and anti-GAPDH (Sigma).

Quantitative RT-PCR. Quantitative PCR was performed to measure the relative mRNA levels using Platinum SYBR Green kit (Invitrogen). Samples were normalized with β-tubulin and actin expression.

***Cre-adenovirus* and GalN/ TNFα Injection.** *Cre-adenovirus* was injected at 2×10^9 pfu/mL in 0.15 mL sterile saline into adult mice via retro-orbital sinus using a 27- to 29-gauge needle. The mice were housed for a week before TNFα/GalN injection. The TNFα-induced liver toxicity experiments were performed as described (51). TNFα was administered via retro-orbital sinus. Blood was collected at 6 h and 24 h respectively. Serum was separated and analyzed for aminotransferase activities.

Isolation and Culture of Primary Mouse Hepatocytes and MEF Cells. Primary hepatocytes were isolated by a two-step collagenase perfusion of the liver (63) from 1- to 2-month-old mice. MEF cells were isolated from E12.5–E14.5 embryos and cultured in DMEM containing 10% FBS.

Apoptosis and Proliferation Assay. Apoptosis assays of MEF cells were performed by flow cytometry after staining the cells with annexin-V-FITC (Pharmingen) and propidium iodide (Roche) following treatment with 10 ng/mL TNFα and 10 μg/mL cycloheximide for 16 h. Hepatocytes were treated with 30 ng/mL TNFα and 10 μg/mL cycloheximide for 8 h, and fragmented DNA were determined with the Cell Death Detection ELISA Kit (Roche). Proliferation was assessed by the percentage of Ki67- or BrdU-positive cells.

Adenoviral Infection and Luciferase Assay. Luciferase activity was measured 24–36 h after transfection according to the Dual-Luciferase Reporter Assay System (Promega). The histograms are presented as the average ± SD from three independent transfections. For adenoviral infection, primary hepatocytes or MEF cells were incubated with *Cre- adenovirus* at 1×10^9 pfu/mL for 2 h in suspension, and analyzed 48–72 h later.

ACKNOWLEDGMENTS. We thank the Yang Laboratory members for stimulating discussions during the course of the work; Drs. Randy Johnson and Dae-Sik Lim for sharing unpublished results; Drs. Zheng-Gang Liu and Xinwei Wang for insights into TNF signaling and liver tumors; and Julia Fekecs for help in preparing the figures. This work is supported by the Intramural Research Program of the National Human Genome Research Institute. (Y. Y.) and the Welch Foundation grant I-1603 (J. J.).

1. Twitty VC, Schwind JL (1931) The growth of eyes and limbs transplanted heteroplastically between two species of Amybystoma. *J Exp Zool* 59:61–86.

2. Wolpert L (1981) Cellular basis of skeletal growth during development. *Br Med Bull* 37:215–219.

3. Müller-Sieburg CE, Cho RH, Sieburg HB, Kupriyanov S, Riblet R (2000) Genetic control of hematopoietic stem cell frequency in mice is mostly cell autonomous. *Blood* 95: 2446–2448.
4. Robin C, et al. (2006) An unexpected role for IL-3 in the embryonic development of hematopoietic stem cells. *Dev Cell* 11:171–180.
5. Edgar BA (2006) From cell structure to transcription: Hippo forges a new path. *Cell* 124:267–273.
6. Pan D (2007) Hippo signaling in organ size control. *Genes Dev* 21:886–897.
7. Zhang L, Yue T, Jiang J (2009) Hippo signaling pathway and organ size control. *Fly (Austin)* 3:68–73.
8. Harvey KF, Pfleger CM, Hariharan IK (2003) The Drosophila Mst ortholog, hippo, restricts growth and cell proliferation and promotes apoptosis. *Cell* 114:457–467.
9. Jia J, Zhang W, Wang B, Trinko R, Jiang J (2003) The Drosophila Ste20 family kinase dMST functions as a tumor suppressor by restricting cell proliferation and promoting apoptosis. *Genes Dev* 17:2514–2519.
10. Pantalacci S, Tapon N, Léopold P (2003) The Salvador partner Hippo promotes apoptosis and cell-cycle exit in Drosophila. *Nat Cell Biol* 5:921–927.
11. Udan RS, Kango-Singh M, Nolo R, Tao C, Halder G (2003) Hippo promotes proliferation arrest and apoptosis in the Salvador/Warts pathway. *Nat Cell Biol* 5: 914–920.
12. Wu S, Huang J, Dong J, Pan D (2003) hippo encodes a Ste-20 family protein kinase that restricts cell proliferation and promotes apoptosis in conjunction with salvador and warts. *Cell* 114:445–456.
13. Justice RW, Zilian O, Woods DF, Noll M, Bryant PJ (1995) The Drosophila tumor suppressor gene warts encodes a homolog of human myotonic dystrophy kinase and is required for the control of cell shape and proliferation. *Genes Dev* 9:534–546.
14. Tapon N, et al. (2002) Salvador promotes both cell cycle exit and apoptosis in Drosophila and is mutated in human cancer cell lines. *Cell* 110:467–478.
15. Xu T, Wang W, Zhang S, Stewart RA, Yu W (1995) Identifying tumor suppressors in genetic mosaics: The Drosophila lats gene encodes a putative protein kinase. *Development* 121:1053–1063.
16. Lai ZC, et al. (2005) Control of cell proliferation and apoptosis by mob as tumor suppressor, mats. *Cell* 120:675–685.
17. Huang J, Wu S, Barrera J, Matthews K, Pan D (2005) The Hippo signaling pathway coordinately regulates cell proliferation and apoptosis by inactivating Yorkie, the Drosophila homolog of YAP. *Cell* 122:421–434.
18. Harvey K, Tapon N (2007) The Salvador-Warts-Hippo pathway—an emerging tumour-suppressor network. *Nat Rev Cancer* 7:182–191.
19. Zeng Q, Hong W (2008) The emerging role of the hippo pathway in cell contact inhibition, organ size control, and cancer development in mammals. *Cancer Cell* 13: 188–192.
20. Dong J, et al. (2007) Elucidation of a universal size-control mechanism in Drosophila and mammals. *Cell* 130:1120–1133.
21. Zhang L, et al. (2008) The TEAD/TEF family of transcription factor Scalloped mediates Hippo signaling in organ size control. *Dev Cell* 14:377–387.
22. Oh H, Irvine KD (2008) In vivo regulation of Yorkie phosphorylation and localization. *Development* 135:1081–1088.
23. Wu S, Liu Y, Zheng Y, Dong J, Pan D (2008) The TEAD/TEF family protein Scalloped mediates transcriptional output of the Hippo growth-regulatory pathway. *Dev Cell* 14:388–398.
24. Goulev Y, et al. (2008) SCALLOPED interacts with YORKIE, the nuclear effector of the hippo tumor-suppressor pathway in Drosophila. *Curr Biol* 18:435–441.
25. Zhao B, et al. (2007) Inactivation of YAP oncoprotein by the Hippo pathway is involved in cell contact inhibition and tissue growth control. *Genes Dev* 21: 2747–2761.
26. Camargo FD, et al. (2007) YAP1 increases organ size and expands undifferentiated progenitor cells. *Curr Biol* 17:2054–2060.
27. Hao Y, Chun A, Cheung K, Rashidi B, Yang X (2008) Tumor suppressor LATS1 is a negative regulator of oncogene YAP. *J Biol Chem* 283:5496–5509.
28. Zender L, et al. (2006) Identification and validation of oncogenes in liver cancer using an integrative oncogenomic approach. *Cell* 125:1253–1267.
29. Overholtzer M, et al. (2006) Transforming properties of YAP, a candidate oncogene on the chromosome 11q22 amplicon. *Proc Natl Acad Sci USA* 103:12405–12410.
30. Steinhardt AA, et al. (2008) Expression of Yes-associated protein in common solid tumors. *Hum Pathol* 39:1582–1589.
31. Zhang H, et al. (2009) TEAD transcription factors mediate the function of TAZ in cell growth and epithelial-mesenchymal transition. *J Biol Chem* 284:13355–13362.
32. Zhao B, et al. (2008) TEAD mediates YAP-dependent gene induction and growth control. *Genes Dev* 22:1962–1971.
33. Cao X, Pfaff SL, Gage FH (2008) YAP regulates neural progenitor cell number via the TEA domain transcription factor. *Genes Dev* 22:3320–3334.
34. Ota M, Sasaki H (2008) Mammalian Tead proteins regulate cell proliferation and contact inhibition as transcriptional mediators of Hippo signaling. *Development* 135:4059–4069.
35. Hayashi S, Tenzen T, McMahon AP (2003) Maternal inheritance of Cre activity in a Sox2Cre deleter strain. *Genesis* 37:51–53.
36. Logan M, et al. (2002) Expression of Cre recombinase in the developing mouse limb bud driven by a Prxl enhancer. *Genesis* 33:77–80.
37. Hayashi S, McMahon AP (2002) Efficient recombination in diverse tissues by a tamoxifen-inducible form of Cre: A tool for temporally regulated gene activation/inactivation in the mouse. *Dev Biol* 244:305–318.
38. Soriano P (1999) Generalized lacZ expression with the ROSA26 Cre reporter strain. *Nat Genet* 21:70–71.
39. Postic C, Magnuson MA (2000) DNA excision in liver by an albumin-Cre transgene occurs progressively with age. *Genesis* 26:149–150.
40. Takigawa Y, Brown AM (2008) Wnt signaling in liver cancer. *Curr Drug Targets* 9: 1013–1024.
41. Mishra L, et al. (2009) Liver stem cells and hepatocellular carcinoma. *Hepatology* 49: 318–329.
42. MacDonald BT, Tamai K, He X (2009) Wnt/beta-catenin signaling: Components, mechanisms, and diseases. *Dev Cell* 17:9–26.
43. Roskams T (2006) Liver stem cells and their implication in hepatocellular and cholangiocarcinoma. *Oncogene* 25:3818–3822.
44. Thorgeirsson SS (1996) Hepatic stem cells in liver regeneration. *FASEB J* 10:1249–1256.
45. Fausto N (1990) Hepatocyte differentiation and liver progenitor cells. *Curr Opin Cell Biol* 2:1036–1042.
46. Shachaf CM, et al. (2004) MYC inactivation uncovers pluripotent differentiation and tumour dormancy in hepatocellular cancer. *Nature* 431:1112–1117.
47. Fausto N, Campbell JS (2003) The role of hepatocytes and oval cells in liver regeneration and repopulation. *Mech Dev* 120:117–130.
48. Fausto N, Laird AD, Webber EM (1995) Liver regeneration. 2. Role of growth factors and cytokines in hepatic regeneration. *FASEB J* 9:1527–1536.
49. Wullaert A, van Loo G, Heyninck K, Beyaert R (2007) Hepatic tumor necrosis factor signaling and nuclear factor-kappaB: Effects on liver homeostasis and beyond. *Endocr Rev* 28:365–386.
50. Pobezinskaya YL, et al. (2008) The function of TRADD in signaling through tumor necrosis factor receptor 1 and TRIF-dependent Toll-like receptors. *Nat Immunol* 9:1047–1054.
51. Ogasawara J, et al. (1993) Lethal effect of the anti-Fas antibody in mice. *Nature* 364: 806–809.
52. Leu JI, Crissey MA, Taub R (2003) Massive hepatic apoptosis associated with TGF-beta1 activation after Fas ligand treatment of IGF binding protein-1-deficient mice. *J Clin Invest* 111:129–139.
53. Yang YA, Zhang GM, Feigenbaum L, Zhang YE (2006) Smad3 reduces susceptibility to hepatocarcinoma by sensitizing hepatocytes to apoptosis through downregulation of Bcl-2. *Cancer Cell* 9:445–457.
54. Bennett FC, Harvey KF (2006) Fat cadherin modulates organ size in Drosophila via the Salvador/Warts/Hippo signaling pathway. *Curr Biol* 16:2101–2110.
55. Silva E, Tsatskis Y, Gardano L, Tapon N, McNeill H (2006) The tumor-suppressor gene fat controls tissue growth upstream of expanded in the hippo signaling pathway. *Curr Biol* 16:2081–2089.
56. Willecke M, et al. (2006) The fat cadherin acts through the hippo tumor-suppressor pathway to regulate tissue size. *Curr Biol* 16:2090–2100.
57. Stanger BZ, Tanaka AJ, Melton DA (2007) Organ size is limited by the number of embryonic progenitor cells in the pancreas but not the liver. *Nature* 445:886–891.
58. Verheyden JM, Sun X (2008) An Fgf/Gremlin inhibitory feedback loop triggers termination of limb bud outgrowth. *Nature* 454:638–641.
59. Scherz PJ, Harfe BD, McMahon AP, Tabin CJ (2004) The limb bud Shh-Fgf feedback loop is terminated by expansion of former ZPA cells. *Science* 305:396–399.
60. Parkin DM, Bray F, Ferlay J, Pisani P (2001) Estimating the world cancer burden: Globocan 2000. *Int J Cancer* 94:153–156.
61. Alison MR, Lovell MJ (2005) Liver cancer: The role of stem cells. *Cell Prolif* 38:407–421.
62. Barrow JR, et al. (2003) Ectodermal Wnt3/beta-catenin signaling is required for the establishment and maintenance of the apical ectodermal ridge. *Genes Dev* 17:394–409.
63. Sun R, Jaruga B, Kulkarni S, Sun H, Gao B (2005) IL-6 modulates hepatocyte proliferation via induction of HGF/p21cip1: Regulation by SOCS3. *Biochem Biophys Res Commun* 338:1943–1949.